KERNFORSCHUNGSZENTRUM

KARLSRUHE

Juni 1977 KFK 2370

Institut für Neutronenphysik und Reaktortechnik
Projekt Schneller Brüter

Analysis of Experimental Fission Gas Behavior Data in Fast Reactor Fuel under Steady State and Transient Conditions

E. A. Fischer

GESELLSCHAFT
FÜR
KERNFORSCHUNG M.B.H.

KARLSRUHE

Als Manuskript vervielfältigt

Für diesen Bericht behalten wir uns alle Rechte vor

GESELLSCHAFT FÜR KERNFORSCHUNG M. B. H.

KARLSRUHE

KERNFORSCHUNGSZENTRUM KARLSRUHE

KFK 2370

Institut für Neutronenphysik und Reaktortechnik

Projekt Schneller Brüter

Analysis of Experimental Fission Gas Behavior Data in Fast Reactor Fuel under Steady State and Transient Conditions

E.A. Fischer

Gesellschaft für Kernforschung mbH, Karlsruhe

Abstract

To assess the utility of the computer programs LANGZEIT and KURZZEIT for the prediction of the fission gas behavior in LMFBR accident analysis, the input parameters were reassessed, a systematic comparison of the results with experimental data was carried out, and the model was further developed to include the diffusion of gas bubbles in a thermal gradient.

The empirical relation by Dutt was used for a comparison of the predicted gas release with experimental data. In addition, a comparison with data obtained in the fuel irradiation program of the Debenelux Fast Breeder Project was also carried out. The LANGZEIT results obtained using the new input parameters are consistent with experimental data for burn up values above 20000 MWd/to. For lower burn up, LANGZEIT overestimates the gas release, because it considers the gas at grain boundaries as released. (An improved model is now available.)

The program KURZZEIT was used to analyse transient gas release laboratory experiments carried out at HEDL. For this purpose, the effect of bubble diffusion in a thermal gradient had to be included in the model, because it plays an important role in those experiments. If reasonable values for the bubble diffusion coefficient are used, the model predicts correctly the time needed until complete gas release in the HEDL experiment, but not the details of the release history.

Analyse experimenteller Ergebnisse zur stationären und transienten Spaltgasfreisetzung im Schnellbrüter-Brennstoff

Zusammenfassung

Es sollen Aussagen darüber gewonnen werden, wie gut die Programme LANGZEIT und KURZZEIT zur Vorhersage des Spaltgasverhaltens in der Störfallanalyse für abgebrannte Schnellbrüter-Cores verwendbar sind. Dazu wurden a) die Eingabeparameter auf den neuesten Stand gebracht, b) systematische Vergleiche mit experimentellen Daten über das Langzeit- und Kurzzeitverhalten durchgeführt und c) das Modell durch Berücksichtigung der Blasendiffusion im thermischen Gradienten erweitert.

Für den Vergleich der berechneten stationären Gasfreisetzung mit experimentellen Daten wurde einmal die Formel von Dutt herangezogen, die eine Anpassung an Bestrahlungsexperimente am EBR-2 darstellt. Daneben wurden auch die Ergebnisse aus dem Bestrahlungsprogramm des Schnellbrüter-Projektes verwendet. Für Abbrände über etwa 20000 Mwd/to sind die LANGZEIT-Ergebnisse mit den neuen Parametern konsistent mit den experimentellen Daten. Für kürzere Abbrände überschätzt LANGZEIT die Freisetzung. Diese Abweichung ist darauf zurückzuführen, daß das Modell keine Aussage über das Verhalten des Gases an den Korngrenzen macht. (Ein verbessertes Modell liegt jetzt vor.)

Mit dem Programm KURZZEIT wurden Labor-Experimente von HEDL zur transienten Gasfreisetzung analysiert. Die Blasendiffusion im thermischen Gradienten, die bisher in KURZZEIT nicht berücksichtigt war, wurde modelliert und in das Programm eingebaut, da sie für diese Experimente eine wesentliche Rolle spielt. Mit plausiblen Werten für den Blasen-Diffusionskoeffizienten wird die Zeit bis zur vollständigen Gasfreisetzung, aber nicht das detaillierte Freisetzungsverhalten richtig wiedergegeben.

TABLE OF CONTENTS

1. INTRODUCTION

The analysis of hypothetical accidents for irradiated liquid-metal fast breeder reactor (LMFBR) cores requires an adequate description of the fission gas behavior in the fuel pin. Codes for gas behavior were developped at several laboratories, for example, GRASS /1/ and FRAS /2/ at Argonne National Laboratory. However, these codes are based on rather detailed models and require long running times on the computer. At Karlsruhe, a gas behavior model developped by Ronchi and Matzke at EURATOM /3,4/ was adopted. Two computer routines based on this model are available: LANGZEIT for the steady state, and KURZZEIT for the transient behavior /5/. The model is simple enough to be used in routine calculations, involving as many as a few thousand fuel nodes in the reactor. However, what is missing is a systematic check against available experimental data, and it is the purpose of this work to carry out such a check, both for the steady state gas release, where data from fuel irradiation programs were available /6,7/ and for transient gas release, where there is interesting information from laboratory experiments carried out at Hanford Engineering Development Laboratory (HEDL) /8/. In addition, the input parameters were updated, and the model was further developped to include the effect of biased migration of gas bubbles in a thermal gradient. This effect is important for the description of the transient gas release experiments.

2. MODEL ASSUMPTIONS

2.1 Comments on the Model by Ronchi and Matzke

The fission gas behavior model by Ronchi and Matzke has been described in detail in the literature /3,4,5/. In brief, it is based on the following assumptions. The gas produced by fission can be retained in the lattice of the oxide fuel in dynamic solution, i.e. the gas atoms occupy unstable interstitial or vacancy positions, or are periodically reinjected in these sites by collisions with fission fragments. The gas retained in the fuel is subject to three main processes, namely precipitation of gas into intragranular bubbles, resolution of bubble gas in the lattice due to

collisions with fission fragments, and finally, the gas in the fuel lattice undergoes diffusion to the grain boundaries, which are assumed to be permanent sinks. The equations describing these processes are given in the Appendix.

In the version of the model used for this work, it was assumed that the gas precipitated at grain boundaries is released into the central channel, thus neglecting the retention of gas in intergranular pores. At present, a new version of LANGZEIT is practically completed, which includes a model for the behavior of gas at grain boundaries, based on the mathematical percolation theory /6/.

2.2 Migration of Gas Bubbles

The programs LANGZEIT/KURZZEIT, in the original version, did not take account of the diffusion of fission gas bubbles. This process, which is considered the dominant mechanism for gas release in the codes GRASS /1/ and FRAS /2/, is certainly present, but there is still a large uncertainty as to the magnitude of this effect. Poeppel /1/ estimated the diffusion coefficient on the basis of two different mechanisms, namely surface diffusion, and vapor phase diffusion. He found that the first process is by far the dominant one, and he obtained the following value for the bubble diffusion coefficient

$$D_b = \frac{0.384 \times 10^{-24}}{r^4} \exp(-108000/RT) \qquad (1)$$

where the bubble radius r is in cm, RT in cal/mol.

To assess the influence of bubble diffusion on gas release, the paths which bubbles travel, either by random motion, or by biased migration in a thermal gradient, will now be estimated, using Poeppel's value for D_b. For random motion of gas bubbles, one has

$$\Delta x = 6 D_b t \qquad (2)$$

where t is the diffusion time. On the other hand, the migration speed of a bubble moving in a thermal gradient is /1/

$$v_b = D_b \frac{4\pi r^3}{3\Omega} \frac{Q^*}{RT} \frac{3}{2} \frac{\nabla T}{T} \qquad (3)$$

where Ω is the molecular volume in solid UO_2, assumed to be 4.09×10^{-23} cm^3, and the activation energy Q^* is taken to be 10^5 cal/mol, as was suggested by Poeppel.

With these data, it is obvious that bubble migration is negligibly small in unrestructured fuel, i.e. at temperatures below 1300°C. However, at higher temperatures, bubbles migrate at a considerable speed. To estimate the order of magnitude, assume a temperature of 1800°C, a bubble radius of 10 nm, a grain size of 10 µm, and a temperature gradient of 4000°C/cm. Then, the bubbles move at a speed of 1.1×10^{-5} cm/sec in the gradient, and thus reach the grain boundary after 90 seconds. In comparison, the distances travelled by random migration are several orders of magnitude lower.

On the basis of these estimates, one expects that biased migration of gas bubbles is an important mechanism for quick gas release in high-temperature fuel, both under steady state and transient conditions. Considering first the steady state case, one observes, however, that the mechanism of the Ronchi-Matzke model, namely diffusion of atomic gas to grain boundaries, also predicts quick gas release at high temperatures. Thus, it turns out that the results of steady state calculations with LANGZEIT do not depend strongly on whether bubble migration is included or not (see section 4.3). It was, therefore, decided to neglect this effect in the reference version of LANGZEIT.

The situation is different for the case of temperature transients with irradiated fuel. By the time the gas containing unrestructured fuel reaches the temperature range where transient gas release is fast enough to be of importance, the gas in dynamic solution has disappeared, due to the process of precipitation in bubbles. Thus, bubble migration is the only important mechanism for transient gas release, and it was necessary to take account of this effect in the analysis of the transient gas behavior.

Therefore, a simple model for bubble migration was included in the KURZZEIT program. It was assumed that the bubbles, which all have the same size in the Ronchi-Matzke model, move with the speed given by Eq. (3). The gas is released as the bubble reaches a grain boundary. No new bubbles are formed during the transient, so that a bubble-free region, increasing in size, is formed. The equations, as used in a new version of KURZZEIT, are given in the Appendix.

As mentioned above, the bubble diffusion coefficient is not well known. Buescher and Meyer /7/ measured the migration velocities of cyclotron-injected helium bubbles in UO_2. These experiments cover the range of bubbles sizes which are important for the present study, and are therefore more interesting than earlier experimental data quoted by Poeppel /1/. The results by Buescher and Meyer can be represented by the bubble diffusion coefficient

$$D_b = \frac{1.19 \times 10^{-22}}{r^3} \exp(-100000/RT) \qquad (4)$$

For a bubble radius of 20 nm, typical for a LANGZEIT calculation, the result of Eq. (4) is about two orders of magnitude lower than the theoretical prediction by Poeppel. As this discrepancy is not explained at present, it was decided to work with a value of average magnitude, which was taken to be 10 % of Poeppel's diffusion coefficient, Eq. (1). It will be demonstrated that the final results are not very sensitive to the value selected.

3. UPDATING OF THE INPUT PARAMETERS

Following suggestions by the authors of the model /3/, some of the input parameters were re-evaluated. First, the gas diffusion coefficient is assumed to be given by the equation (see also the Appendix)

$$D = A \exp(-Q/RT) + D^*$$

The coefficients A = 0.25 and Q = 100000 cal/mol, corresponding to a hypostoichiometric fuel, were retained as used by Bogensberger /5/. The term D^* refers to radiation enhanced diffusion, due to radiation-created defects which act as diffusion carriers. This term was inferred from in-pile self-diffusion measurements by Höh and Matzke /8/. These authors obtained a diffusion coefficient $D^* = 1.7 \times 10^{-16}$ cm^2/sec for UO_2 at 900^oC and at a fission rate of $1.13 \times 10^{13}/cm^3 sec$. This value is by about three orders of magnitude higher than the extrapolated thermal diffusion coefficient, so that radiation-enhanced diffusion becomes the dominant mechanism at lower temperatures. The experimental results are compatible with the theoretical assumption that D^* is proportional to the fission rate. Therefore, D^* was taken proportional to the production rate of fission gas, which is the parameter that defines the fission rate in the Ronchi-Matzke equations. Then, the data lead to the relation $D^* = 4.11 \times 10^{-5}\ \beta$. This radiation-enhanced term determines the gas diffusion in the outer, unrestructured regions of the fuel pellet.

In addition, the resolution parameter η was re-evaluated. This parameter determines the rate of re-ejection of gas atoms from bubbles into the lattice by collision with fission fragments. Following the theory of Nelson /9/, it can be calculated from the number of collisions between gas atoms and fission fragments. One obtains values in the range $\eta = 1$ to $2 \times 10^{-5}/sec$ for a fission rate of $3 \times 10^{13}/cm^3 sec$. According to theory, η should be proportional to the fission rate. It should be noted that experiments by Cornell /10/ and by Marlowe /10/ seem to indicate higher values of η. However, the effect observed in these measurements is probably the sum of re-injection of atoms into the lattice, and a sputtering mechanism which increases the number of bubbles. Therefore, the calculated values seem to be more reliable. In view of the experimental results, the higher calculated value $\eta = 2.0 \times 10^{-5}/sec$ was used; assuming proportionality to the fission rate, one obtains $\eta = 1.83 \times 10^{6}\ \beta$. It must be emphasized that there is still a rather large uncertainty in this parameter.

In the early literature (Appendix 2 of Reference /4/), it was suggested that, at high temperatures, a gas atom ejected from the bubble might not end in an equilibrium position for volume diffusion, but rather be scattered back into the bubble. Thus, η might be much lower at high temperatures (> 1200 to 1300°C). However, this back-scattering effect is not clearly established, and therefore η was taken as independent of temperature for the reference calculations. Nevertheless, the influence of a reduced η at high temperatures was studied in a parameter variation.

For the other parameters, the values used in earlier publications /5/ were retained. The input parameters are summarized in Table 1.

4. INVESTIGATIONS WITH LANGZEIT

4.1 Calculation of the Fission Gas Release during Steady-State Operation as a Function of the Linear Rod Power

The calculation of the fission gas release for a fuel pin at a given linear rod power was performed in the following way: The fuel density, and the pin geometry were defined, as well as the outer clad temperature. Then, the radial temperature profile was calculated, using 9 radial nodes in the fuel pellet. LANGZEIT calculations were performed for each node, and finally the resulting gas release was averaged over the pin cross section.

The data of the fuel pin (Table II) correspond essentially to the fuel specifications for the Debenelux LMFBR prototype SNR 300, with a rather low fuel smeared density of 80 %. The gap is assumed to be closed at operating conditions. A fixed outer clad surface temperature of 479°C was assumed, which corresponds about to the conditions in the axial mid-plane of the SNR-300.

The temperature profile was calculated with MERKUR /11/, a flexible fuel-pin design program which accounts for fuel restructuring, and variations in the fuel thermal conductivity due to restructuring. The fuel thermal conductivity was taken from the Schmid formula /12/ for mixed oxide, assuming O/M = 1.98. MERKUR calculations were run for five different linear rod powers; the resulting temperature profiles are shown in Fig. 1.

The LANGZEIT calculations were performed with the reference set of input parameters, which are listed in Table I. In addition, variations of some of the parameters were also carried out. The results will be discussed, and compared to experimental data, in the following section.

4.2 Comparison with Experimental Gas Release Data

In this section, the LANGZEIT calculations will be compared with experimental results. The formula by Dutt /13/, which was obtained from a correlation of data from EBR-II irradiation tests, was chosen for a comparison. This relation represents the results of a consistent set of experiments, covering a fairly wide range of burnup and linear rod power. In addition, a comparison with the Dutt formula is of interest because authors of accident analysis codes, like HOPE and BREDA, preferred to use it. The specifications for these fuel testsare somewhat different from those of the SNR-300; especially, the smeared fuel density is higher (about 90 %), and it varies over the set of experiments. However, it is expected, and was confirmed by calculations, that the gas release behavior depends very little on the smeared density. Therefore, a valid comparison can be carried out with calculations on the basis of the SNR-300 data. In addition, results from irradiation tests carried out in the frame of the Debenelux Fast Breeder Project will also be used for comparison. The data pertaining to gas release were compiled by Zimmermann /14/. The tests were carried out partly in the thermal reactors FR2 at Karlsruhe, and BR-2 at Mol, and partly in the fast reactors Dounreay and Rapsodie. Thus, they are not a set as consistent as the EBR-II tests. On the other hand, the fuel specifications for these tests were, in general, close to those for the SNR-300.

The calculated and experimental gas release data are compared in Fig. 2 for different values of burn up. The linear rod power is 354 W/cm. The figure shows the relative gas release, which is $g/\beta t$ in terms of the variables in the Appendix. The reference set of input data (Table I) was used in LANGZEIT. The experimental data are the curve corresponding to the Dutt relation, and a band which about characterizes the spread of experimental data quoted by Zimmermann. Similar comparisons are shown for high (440 W/cm) and low linear rod power (251 W/cm) in Fig. 3. For high burn up, the two sets of experimental data are well in agreement, except for the low linear rod power. The calculation is consistent with the experimental data in view of their scatter,

though it is slightly low. Again, the 251 W/cm case in an exception. For low burn up (< 30000 Mwd/to), the Dutt curve is higher than the Zimmermann data. It is not clear whether this is due to different fuel behavior, or due to different techniques for determining the gas content. The calculation tends to overestimate the release, especially at the lower rod powers. This is probably due to the neglection of gas retention in intergranular pores.

In general, one concludes that the LANGZEIT results are in agreement with experiment for high burn up, but they predict too much gas release for low burn up.

4.3 Variation of the Input Parameters

To study the sensitivity of the LANGZEIT results to the input parameters, a variation of the important parameters was carried out for 354 W/cm linear rod power. The results are shown in Fig. 4.

The following cases were calculated:

1 Reference data
2 $\eta(T>1300^{o}C)$ reduced to 20 %
3 bubble diffusion included
4 Q (equation for the diffusion coefficient) reduced to 87000 cal/Mol
5 η reduced by 20 %
6 Fission yield increased to 31 % /14/

Case 2 simulates a reduction of η in the restructured fuel due to a reduced probability for volume diffusion at high temperature (Section 3). The low η leads to a significantly slower rise of the gas release during the early period of burn up. However, this seems to be unrealistic if one considers the presence of bubble migration, which represents a fast release mechanism at high temperatures.

Case 3 shows the effect of including the bubble migration in a thermal gradient. As discussed in Section 2.2, the diffusion coefficient was taken to be 10 % of Poeppel's value. The overall influence on the gas release is rather small, because bubble migration is significant only at high temperatures,

where the model predicts nearly complete release anyway. Thus, the neglection of bubble migration in LANGZEIT does not lead to serious errors.

The other cases correspond to variations of parameters within their range of uncertainty. As can be seen from Fig. 4, the changes of the results are only small, and not significant in view of the uncertainties still present in the experimental data. Therefore, it is justified to use the reference set of input data for further work.

4.4 Results of Parametric Calculations for Gas Release and Swelling

The reference set of input data was used to run a series of LANGZEIT calculations for different linear rod powers, between 150 W/cm and 440 W/cm, which covers the range of interest in fast breeder work. The predicted pellet averaged gas release is shown in Fig. 5. The radial distribution of gas content in the fuel pin is shown in Fig. 6, for two values of burn up. As is to be expected, the gas is concentrated in the outer, unrestructured portion of the fuel. The gas concentration shown includes both the gas in dynamic solution, and in fission gas bubbles. It is of interest to note that the gas concentration in low-powered pins is not much larger than in high-powered ones; however, the gas-bearing region is larger. Fig. 7 shows the steady-state fuel swelling due to fission gas, averaged over the volume of the pellet. The volume changes are lower than predicted in earlier publications /5/, due to the use of new input data.

5. INVESTIGATIONS WITH KURZZEIT

5.1 Comments on the Transient Effects

If the fuel pin undergoes a temperature transient, the gas present in dynamic solution in the unrestructured region of the fuel has an increased tendency to precipitate into existing bubbles. Furthermore, the bubbles grow by capture of vacancies, to obtain the equilibrium pressure with the surface tension of the solid. Therefore, transient fuel swelling takes place due to an increase in the total bubble volume. Bogensberger and Ronchi /5/ discussed this behavior in detail. They also demonstrated that the bubble growth can be well described by the program KURZZEIT, which solves the differential equations in the Appendix for the conditions of a temperature transient.

As the gas-bearing fuel is heated further in the course of a temperature transient (above ∿ 2200°C), biased migration of gas bubbles in the temperature gradient becomes important. To take account of this effect, a simple model for bubble migration (Section 2.2) has been included in the KURZZEIT program. With values of reasonable magnitude for the bubble diffusion coefficient, the migration rates are such that transient release occurs in the order of a few seconds. Therefore, this effect plays a significant role only in rather slow transients (corresponding to a transient overpower accident with less than about 50 ¢/sec), but is negligible in faster excursions.

5.2 Analysis of Laboratory Experiments on Transient Gas Release

In a series of experiments conducted at HEDL /15/, fuel pins irradiated in the EBR-II were subjected to temperature transients in an electrically heated capsule. These experiments provided important information on the fission gas behavior during transient heating. The heating rates were of the order of 200°C per sec. Gas release was measured, and the transient temperature profiles were calculated, taking into account heat conduction, radiation and convection /15/. It was assumed for the heat transfer calculations that the fuel and the capsule are concentric cylinders, and the temperatures may be in error if the fuel was not well centered in the capsule.

One of these tests, FGR-15, is well suitable for theoretical analysis, because complete data under defined conditions of the fuel are available. The fuel was irradiated at 440 W/cm for 45000 MWd/to. The temperature rise, as reported by HEDL /15/, is shown in Fig. 8. Note that the temperature profile is inverted relative to the one in a reactor fuel pin.

To analyse this test, calculations with the program KURZZEIT were carried out, with the input data taken from the LANGZEIT run for 440 W/cm (Fig. 5). The nodal representation of the pin cross section was the same as in LANGZEIT. There was a significant gas content only in the outer 15 % of the fuel radius (compare Fig. 6). The bubble diffusion coefficient was taken to be 10 % of Poeppel's value. Plots of the calculated concentration of gas in bubbles and in dynamic solution are shown in Fig. 9. The values are averages over the gas-bearing region. The figure illustrates that precipitation of the lattice gas in bubbles starts after 10 sec (at ∿ 1600°C), and is completed two seconds later. Still one second later, transient gas release due to biased migration of bubbles becomes important. The release is complete only when the temperature is nearing the melting point.

The experimental and calculated release fractions are plotted in Fig. 10. The release, as calculated with the standard input data starts later, but then proceeds faster than in the experiment. The reason for this deviation is not clear at present. There are, of course, uncertainties in the input parameters. Calculations in which the bubble diffusion coefficient was increased, and decreased by a factor of two serve to estimate the range associated with this uncertainty. However, it definitely cannot explain the observed deviation. Possible reasons are the simplistic features of the model, as neglection of bubble coalescence and release of intergranular gas, or else uncertainties in the data quoted by HEDL /15/, for example in the transient temperature profile. Thus, the KURZZEIT model in its present state reproduces about correctly the time needed till complete gas release, but not the detailed release history.

5.3 Calculation of Transient Swelling and Gas Release

To assess the fuel behavior for different transients, KURZZEIT calculations were carried out assuming a simple adiabatic model for the temperature rise. If the power increases on a constant period, the temperatures are given by the equation

$$T(t) - T_0 = \frac{\chi}{\pi(R^2-R_0^2)\rho_f C_p} \cdot \frac{e^{\alpha t}-\alpha t-1}{\alpha} = C \cdot \frac{e^{\alpha t}-\alpha t-1}{\alpha} \qquad (5)$$

where T_0 is the steady-state temperature, α the inverse period, and χ is the linear rod power. Though this description is rather simplistic, it facilitates calculations for the purpose of comparing different cases. First, calculations were performed for fuel irradiated at 300 W/cm to $\sim$ 80000 MWd/to. The inverse periods were α = 5.4 sec^{-1}, 1.0 sec^{-1} and 0.075 sec^{-1}, which correspond about to initiating ramp rates of 3 - 5 $/sec, 0.5-1 $/sec and 15 ¢/sec. The transient swelling is plotted in Fig. 11 versus the average temperature of the unrestructured fuel. The ramp rate does not greatly influence the swelling, the difference being only about 1.5 % $\Delta V/V$ for the fastest and the slowest ramp. However, the transient release behavior is strongly influenced by the ramp rate. Fig. 12 shows that in the case of a mild overpower transient, represented by α = 0.075 sec^{-1}, most of the gas is released when the fuel reaches the solidus line. On the other hand, the results for α = 5.4 sec^{-1}

demonstrate that in a rapid transient, heating rates are faster than the rate of gas bubble migration, and no substantial release occurs below the solidus. Note that the variable on the abscissa is the temperature of a typical unrestructured node; the dependence on the initial node temperature is small, and was not considered.

In a second set of calculations, the dependence of the transient swelling on the linear rod power was investigated for $\alpha = 1.0\ sec^{-1}$. The swelling as a function of the average unrestructured fuel temperature is larger for the lower power fuel pins. However, one should be careful in the interpretation of these results. If a reactor which contains both high and low powered pins is subject to an overpower transient, fuel melting and pin failure will first occur in the high powered pins.

6. CONCLUSIONS

The computer programs LANGZEIT and KURZZEIT, based on a model by Ronchi and Matzke, were examined as to their utility for the prediction of the fission gas behavior in LMFBR accident analysis. With reassessed input parameters, LANGZEIT calculates steady state gas release fractions which are in satisfactory agreement with experimental data for high burn up, though the release at low burn up is overpredicted by the version used in this work. The KURZZEIT program, which describes the transient gas behavior, had to be modified to include the effect of biased migration of gas bubbles in a thermal gradient. Then, the program predicts the transient gas release history observed in laboratory experiments at HEDL in a qualitative way, but not in detail. Inspite of some shortcomings, the model by Ronchi and Matzke is adequate for use in accident analysis.

ACKNOWLEDGEMENT

The author gratefully acknowledges helpful discussions with Dr. H. G. Bogensberger, Dr. C. Ronchi and Dr. H.J. Matzke.

APPENDIX

Basic Differential Equations for LANGZEIT/KURZZEIT

The differential equations derived by Ronchi and Matzke /3,4,5/ are

$$\dot{c} = \beta - \frac{K}{\sqrt{\beta}} \sqrt{b} \cdot c + C_o\, b - \dot{g}$$

$$\dot{g} = Pos(\dot{c}) \left[1 - \sum_{m=1}^{\infty} \frac{6}{\pi^2 m^2} \exp\left(m^2\pi^2 Dt/a^2\right) \right] + \frac{6cD}{a^2} \sum_{m=1}^{\infty} \exp\left(-m^2\pi^2 Dt/a^2\right)$$

where $D = 0.25 \exp(-Q/T) + D^*$
is the gas diffusion coefficient, and the parameters K and C_o are given by

$$K = D \left(\frac{6\pi n\beta RT}{\sigma}\right)^{1/2} \quad \text{and} \quad C_o = \frac{3}{2} \frac{RT\eta d}{b'\sigma}$$

The nomenclature is

β	production rate of fission gas (mol/cm^{3}sec)
c	concentration of gas in dynamic solution in the lattice (mol/cm^3)
g	gas in sinks (mol/cm^3)
n	density of bubbles (cm^{-3})
σ	surface tension of the fuel (dyn/cm^2)
b'	Van der Waals covolume (cm^3/mol)
d	thickness of the 'surface layer' of the bubble
η	parameter for re-solution or re-ejection of bubble gas
a	average radius of the grain (cm)
$b = \beta t - c - g$	concentration of gas in bubbles (mol/cm^3)

Note that β is given by the equation

$$\beta = \frac{\dot{S}Y}{N} ,$$

where $\dot{S}$ is the fission rate (fissions/cm^{3}sec), Y is the fission yield of the noble gases, and N is Avogadro's number.

In the modified KURZZEIT program, which includes gas bubble diffusion, the gas concentrations b and c are used as the variables. In addition, the bubble density n is now time dependent; n_o is the initial steady-state value. The gas production by fission, and the diffusion of atomic gas to the grain boundaries are completely negligible in the time of interest for KURZZEIT. The equations are then

$$\dot{c} = - 4\pi r n D c + 4\pi n r^2 \frac{d\eta}{b^\tau}$$

$$\dot{b} = - \dot{c} + \frac{\dot{n}}{n} b$$

$$\dot{n} = - \frac{V_b}{Fa} n_o$$

$$r^2 = \frac{3RTb}{8\pi\sigma n}$$

The temperature is a given function of the transient time. r is the temperature-dependent bubble radius, the bubble speed is given by Eq. (3) of Section 2.2. The numerical factor F in the equation for $\dot{n}$ is a geometry factor, to define an average distance across the grain of radius a.

REFERENCES

/1/ R.B. Poeppel
"An Advanced Gas Release and Swelling Subroutine"
Proc. Conf. on Fast Reactor Fuel Element Technology, New Orleans, April 1971

/2/ E.E. Gruber
"Calculation of Transient Fission Gas Release from Oxide Fuels"
ANL-8143 (1974)

/3/ C. Ronchi and H.J. Matzke
J. Nucl. Mater. 45,15 (1972)

/4/ C. Ronchi and H.J. Matzke
"Calculations on the In-Pile Behavior of Fission Gas in Oxide Fuels"
EUR-4877e (1972)

/5/ H.G. Bogensberger and C. Ronchi
Nucl. Technol. 29, 73 (1976)

/6/ C. Ronchi
LWR-Reactor Safety Research Program Progress
Report ANL-7572 (1975)

/7/ B.J. Buescher and R.O. Meyer
J. Nucl. Mater. 48,143 (1973)

/8/ A. Höh and H.J. Matzke
J. Nucl. Mater. 48,157 (1973)

/9/ R.S. Nelson
J. Nucl. Mater. 31,153 (1969)

/10/ R.M. Cornell
J. Nucl. Mater. 36,161 (1970);
M.O. Marlowe, "Fission Gas Re-Solution Rates",
GEAP-12428 (1973)

/11/ L. Steinbock
"Das Brennstab-Auslegungs- und Überwachungssystem MERKUR"
KFK 2163 (1975)

/12/ H.E. Schmidt
"Die Wärmeleitfähigkeit von Uran- und Plutonium-Dioxid bei hohen Temperaturen"
High Temp. High Press. 3,345 (1971)

/13/ D.S. Dutt, D.C. Bullington, R.B. Baker and L.A. Pember
"A Correlated Fission Gas Model for Fast Reactor Fuels"
Trans. Am. Nucl. Soc. 15,198 (1972)

/14/ H. Zimmermann
"Spaltgasverhalten in Oxid-Brennelementen für Schnelle Brüter"
KFK 2057 (1974)

/15/ E.T. Weber, O.D. Slagle and C.A. Hinman
"Laboratory Studies on Melting and Gas Release Behavior of Irradiated Fuel"
Conf. on Fast Reactor Safety, Beverly Hills, California (1974)

TABLE 1

Input Parameters for the Program LANGZEIT

n	number of bubbles per cm^3	$10^{15} cm^{-3}$
b'	van der Waals covolume	49.26 cm^3
σ	surface tension	800 erg/cm^2
d	thickness of the bubbles shell for resolution /9/	10^{-7} cm
η	parameter for the resolution	1.83×10^6 β, s^{-1}
A	pre-exponential term for the gas diffusion coefficient	0.25 cm^2/s
Q	heat of transport for the diffusion process	10^5 cal/mol
D^*	radiation enhanced term for the diffusion coefficient	4.11×10^{-5} β, cm^2/s
Y	fission yield of noble gases	27.5 %

TABLE 2

Data of the Fuel Pin

Fuel Pellet Radius (at operating temperature)	0.262 cm
Clad thickness	0.038 cm
Gap thickness	gap closed
Heat conductance of the gap	0.8 $W/cm^2\ ^oC$
Clad surface temperature	479^oC
Fuel material	$(U,Pu)\ O_{1.98}$
Smeared density of the fuel (cold)	80 % theoretical density
Porosity of unrestructured fuel	0.135
Porosity of the equiaxed grain growth fuel region	0.085
Porosity of the columnar grain growth fuel region	0.050
Isotherm for equiaxed grain growth region	1300^oC
Isotherm for columnar grain growth region	1700^oC

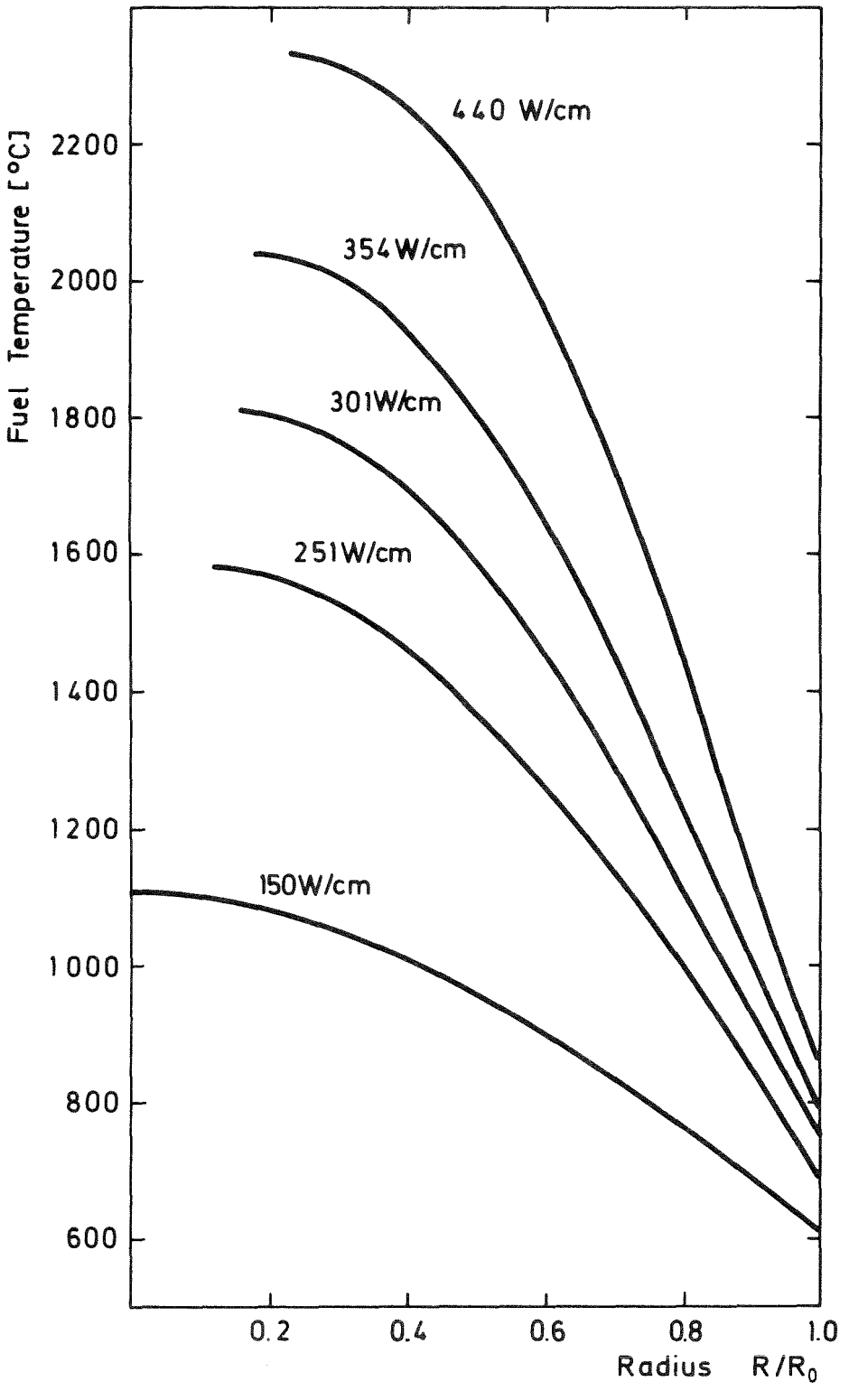

Fig. 1: Radial Temperature Profile in the Fuel Pin

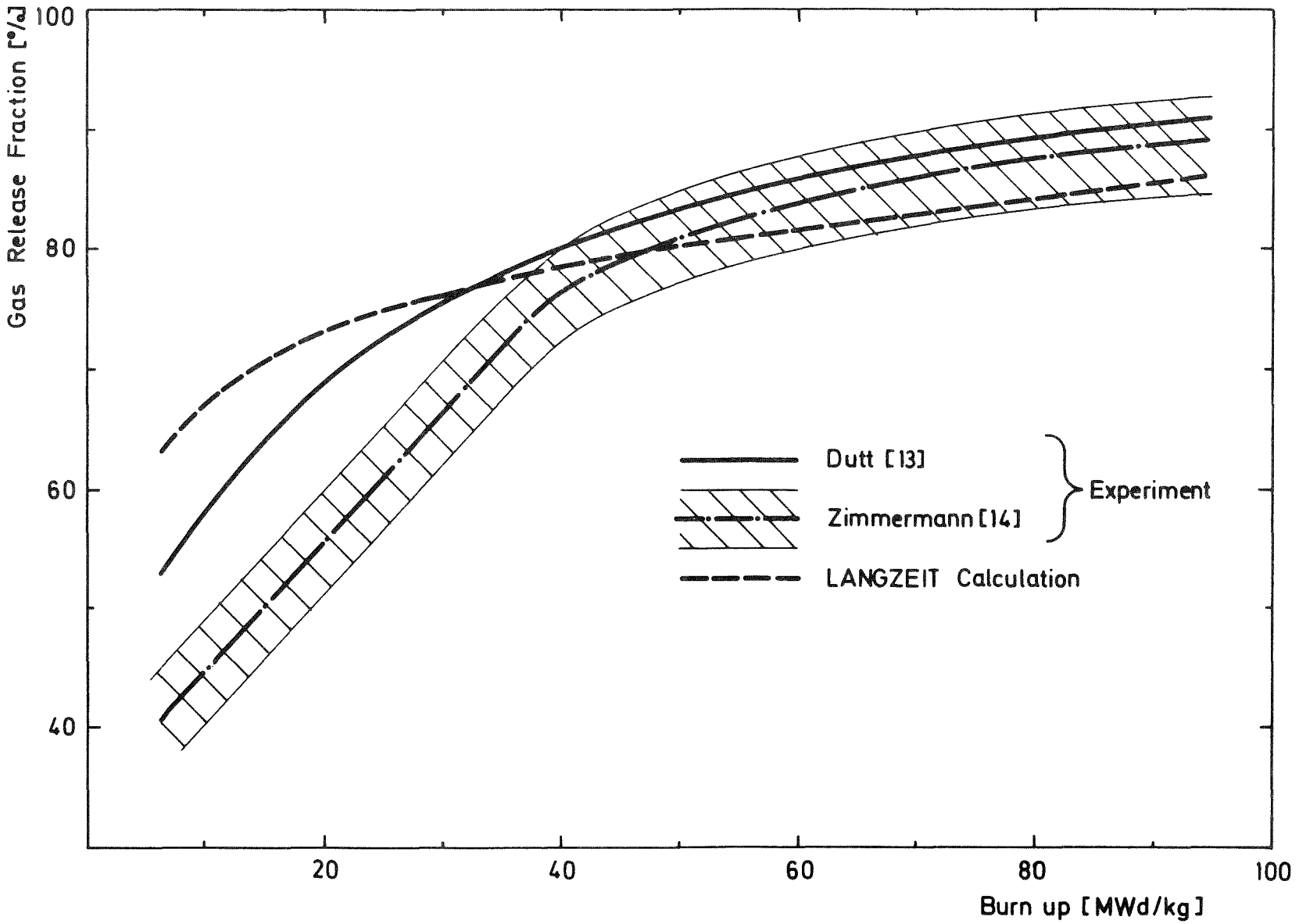

Fig. 2: Experimental and Calculated Fission Gas Release vs. Burn up (354 W/cm)

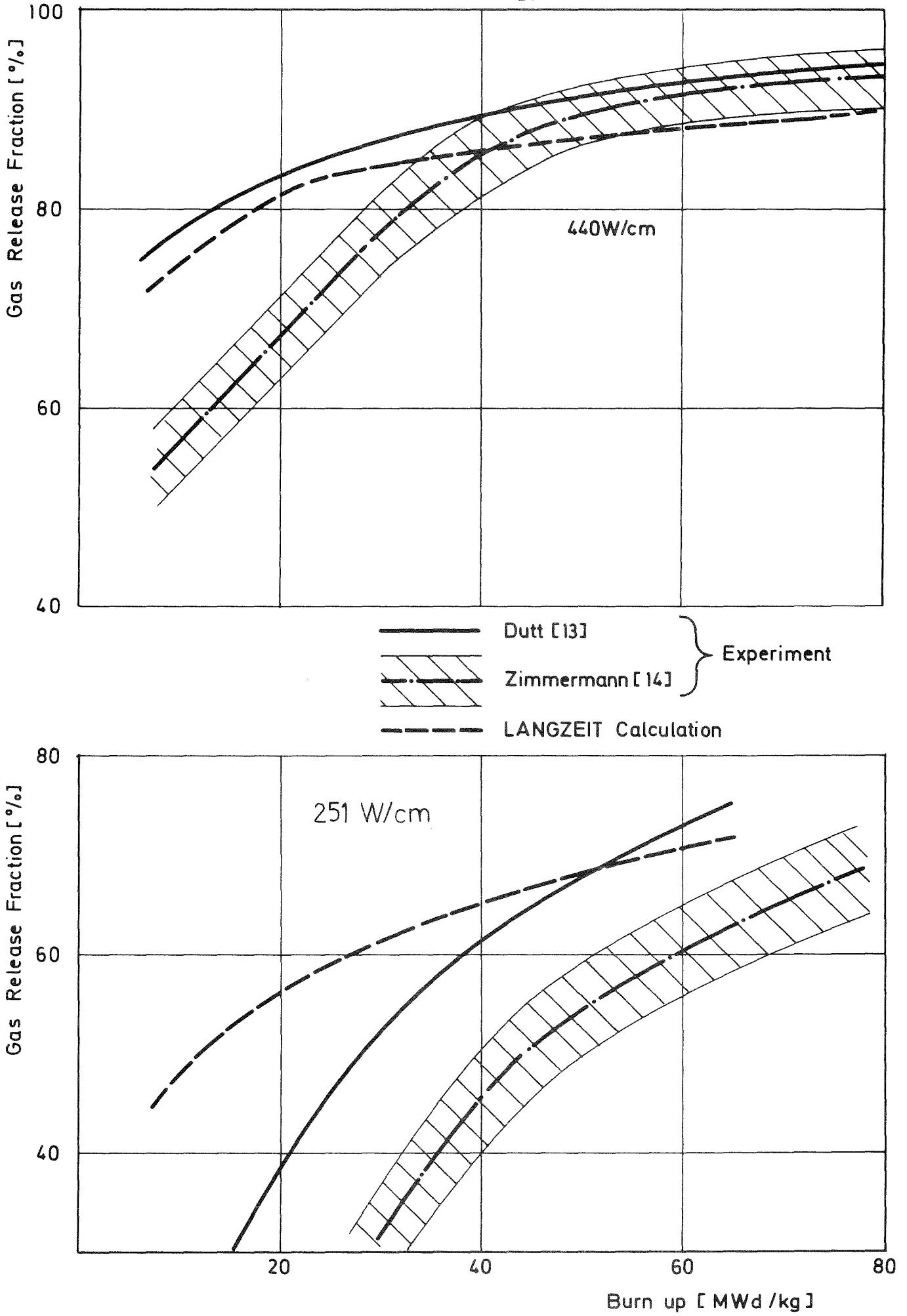

Fig. 3: Experimental and Calculated Fission Gas Release vs. Burn up

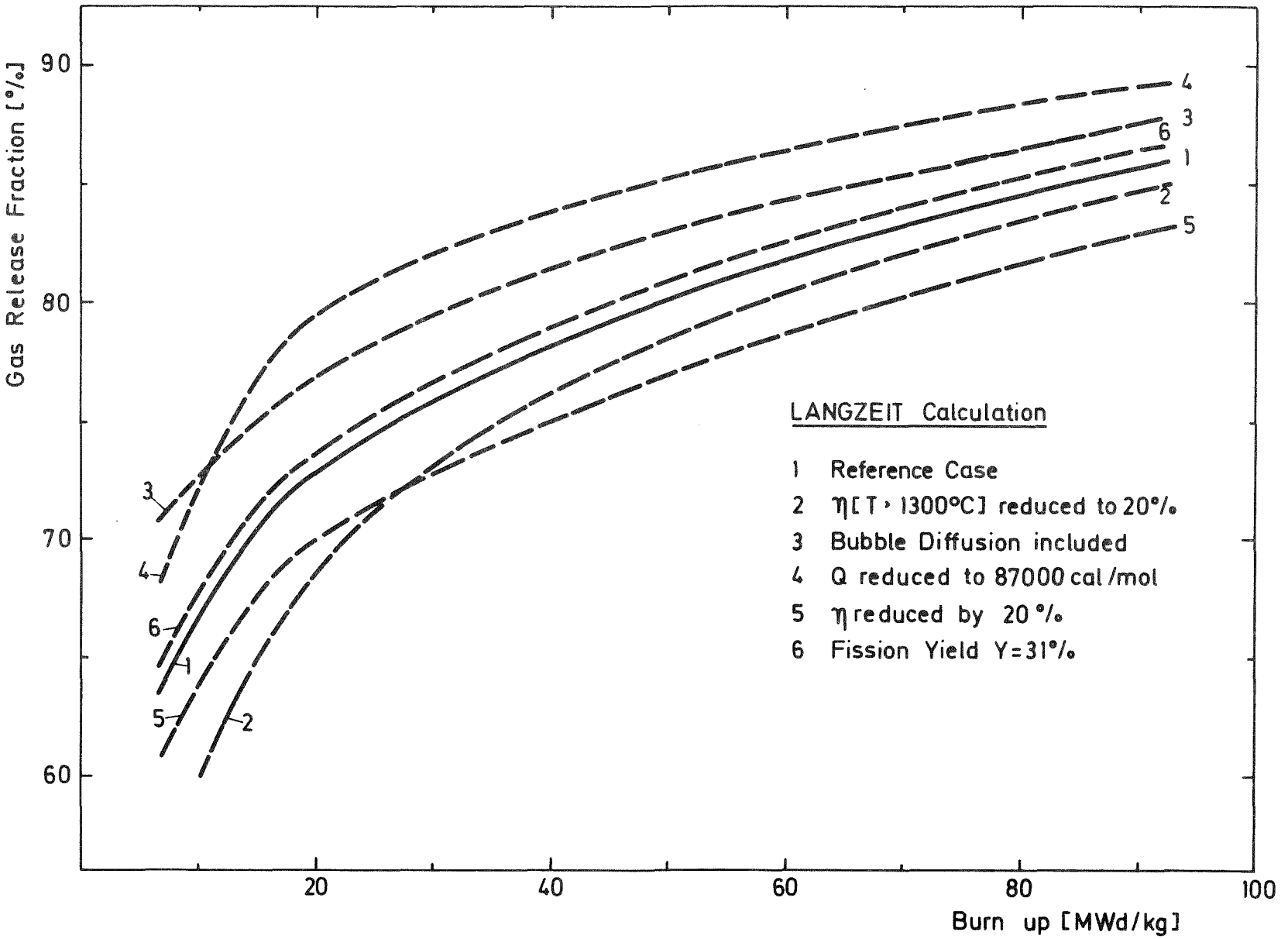

Fig. 4: Calculated Fission Gas Release (354 W/cm): Variation of the Input Parameters

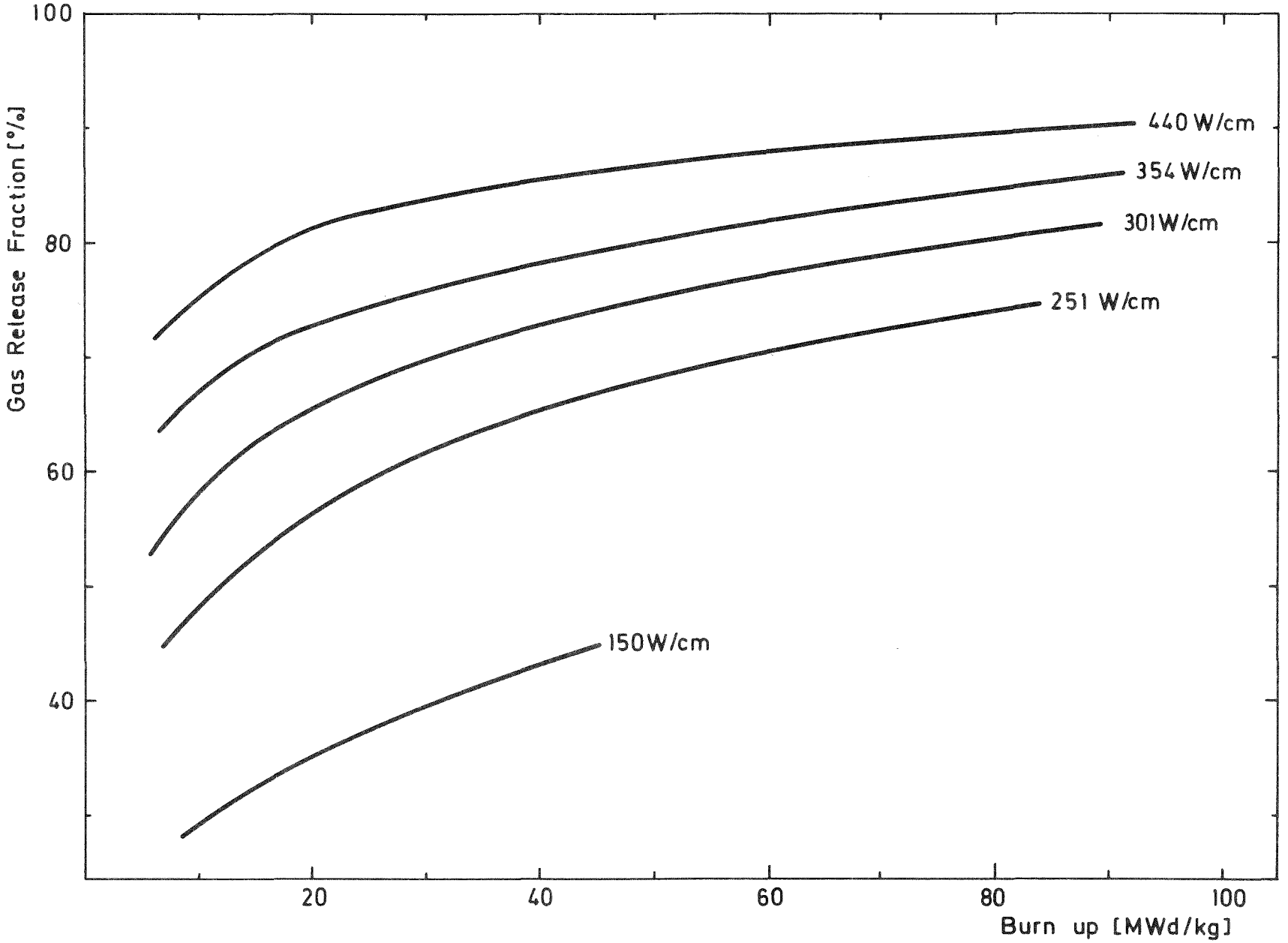

Fig. 5: Calculated Fission Gas Release for Different Linear Rod Powers

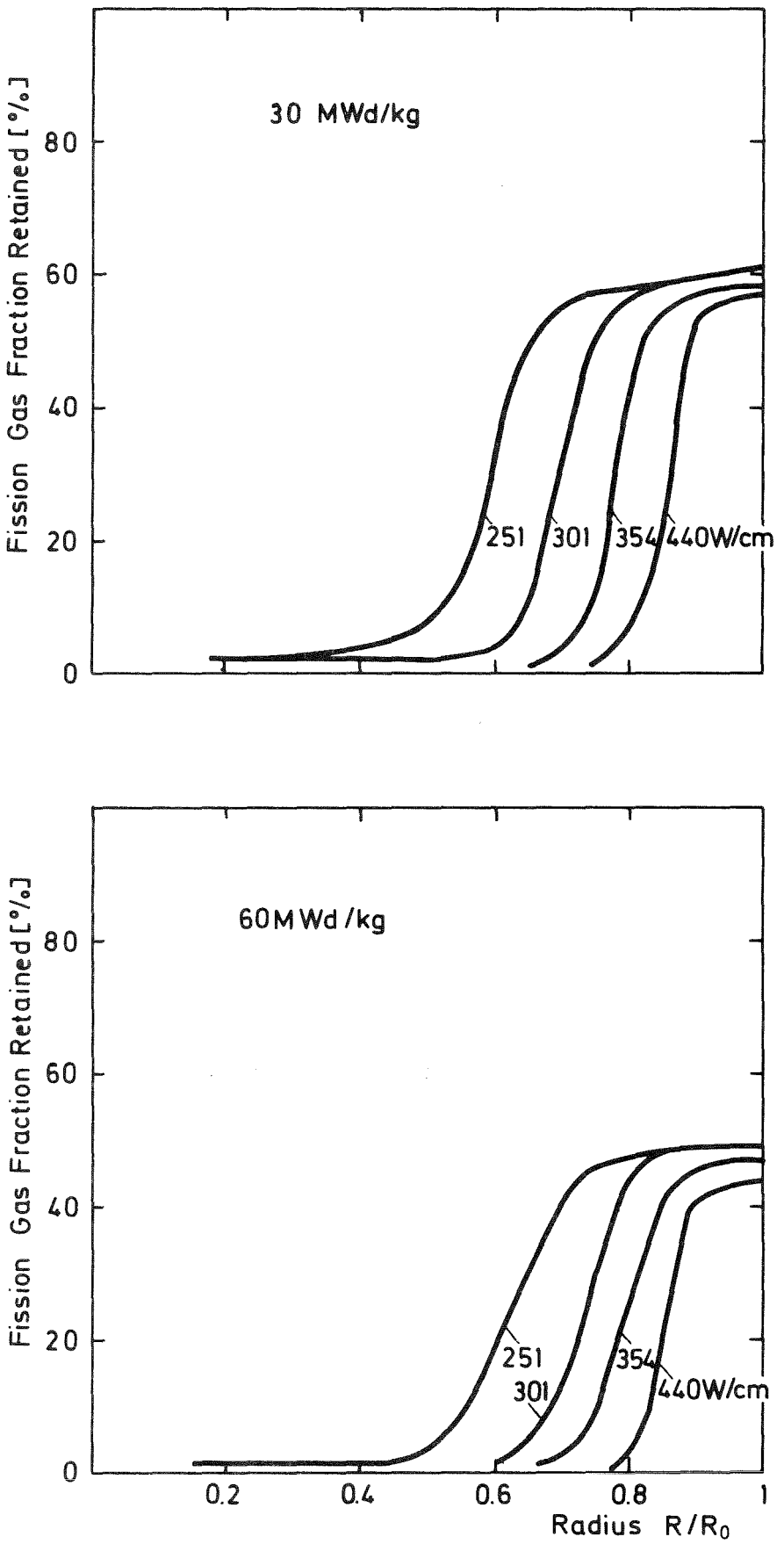

Fig. 6: Radial Distribution of Retained Fission Gas in the Fuel

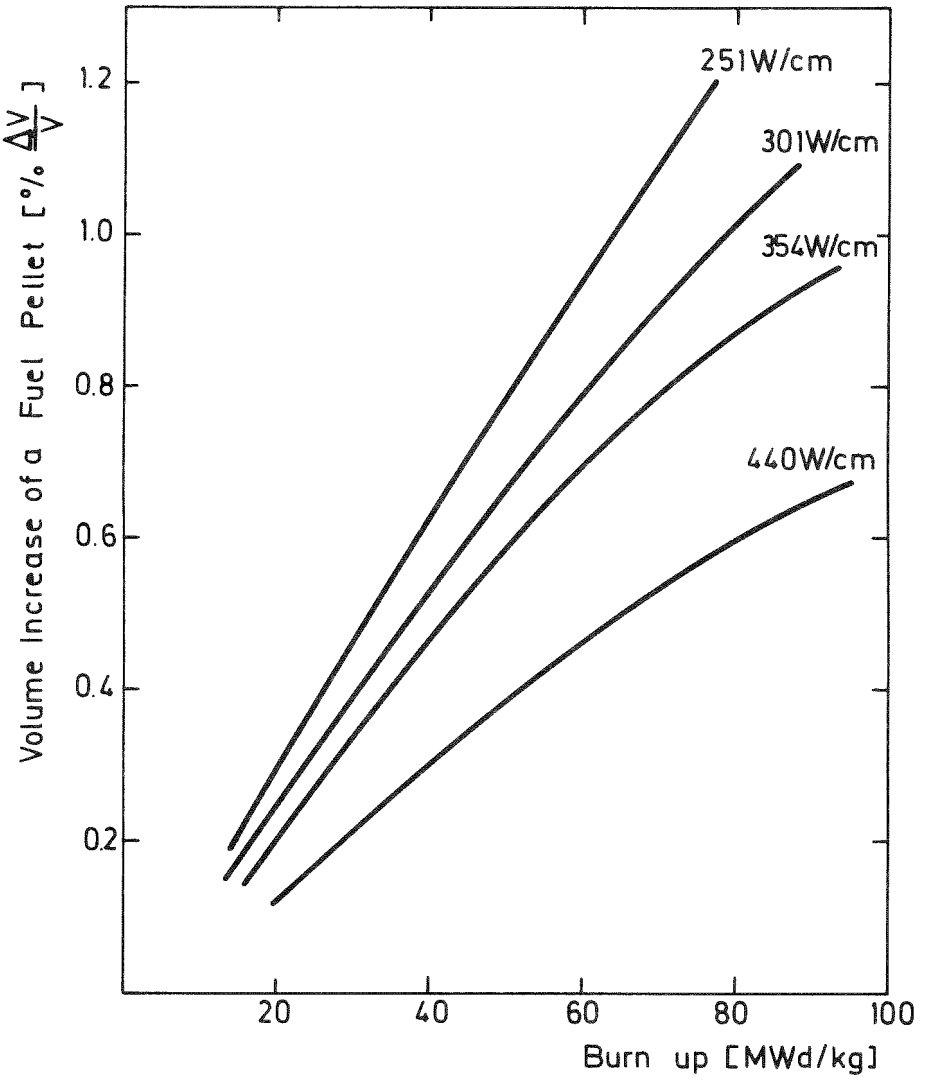

Fig. 7: Steady-State Fuel Swelling due to Fission Gas

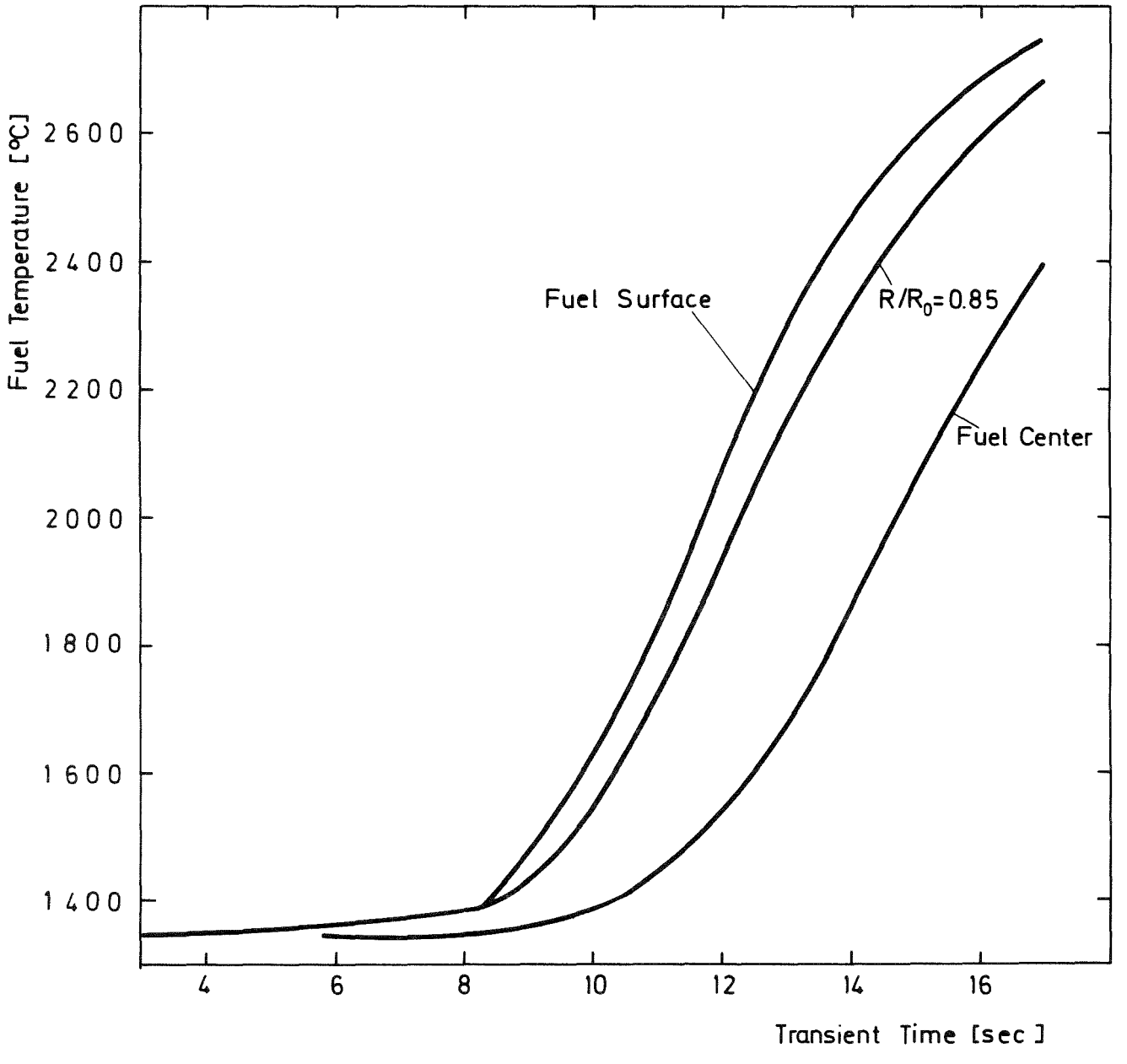

Fig. 8: Transient Fuel Temperature Rise, Test FGR-15

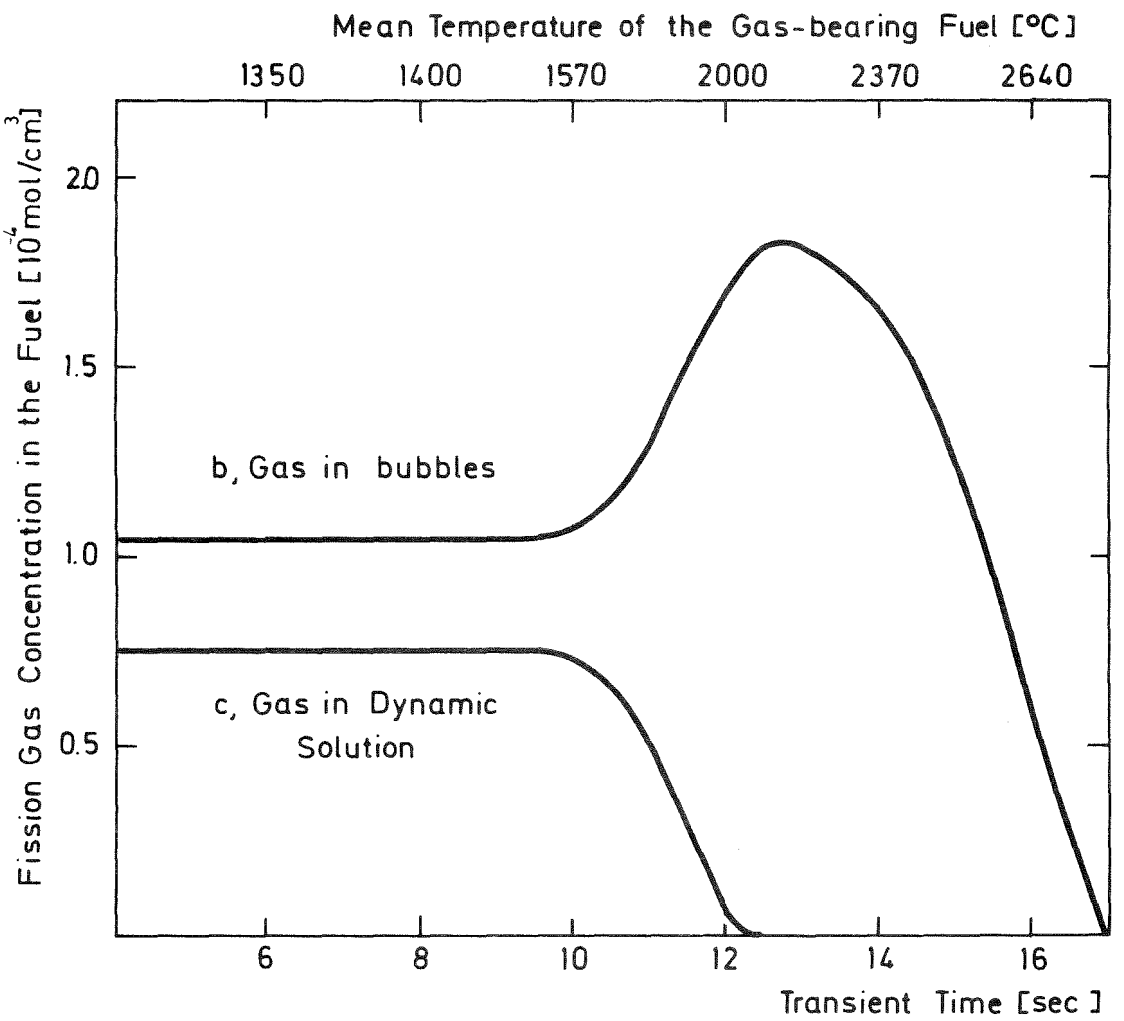

Fig. 9: Fission Gas Concentrations During the Test FGR-15

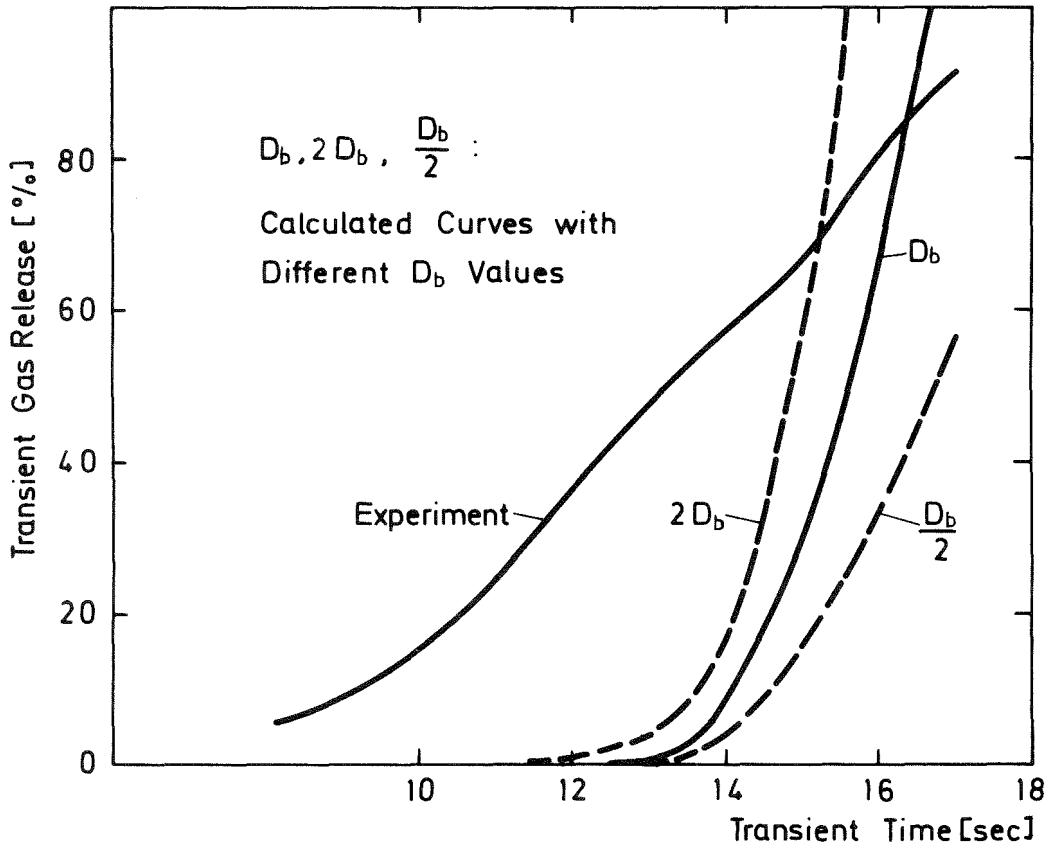

Fig. 10: Transient Fission Gas Release, Test FGR-15
Experiment and Calculations

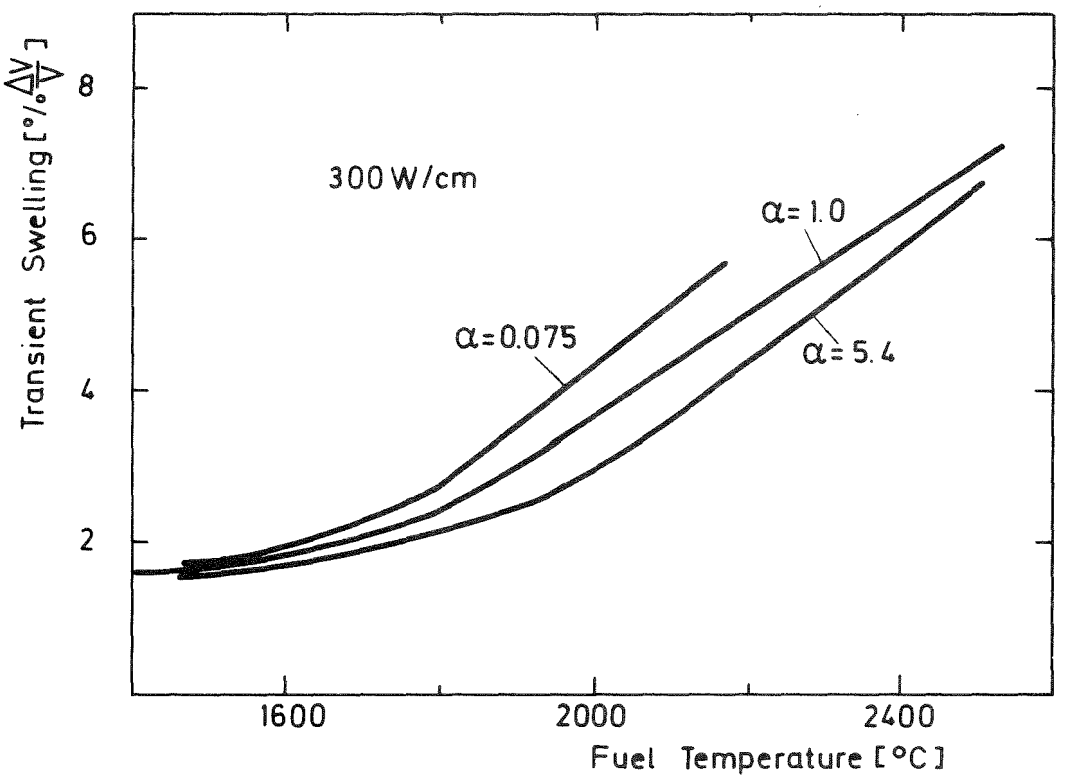

Fig. 11: Transient Fuel Swelling for Different Periods α

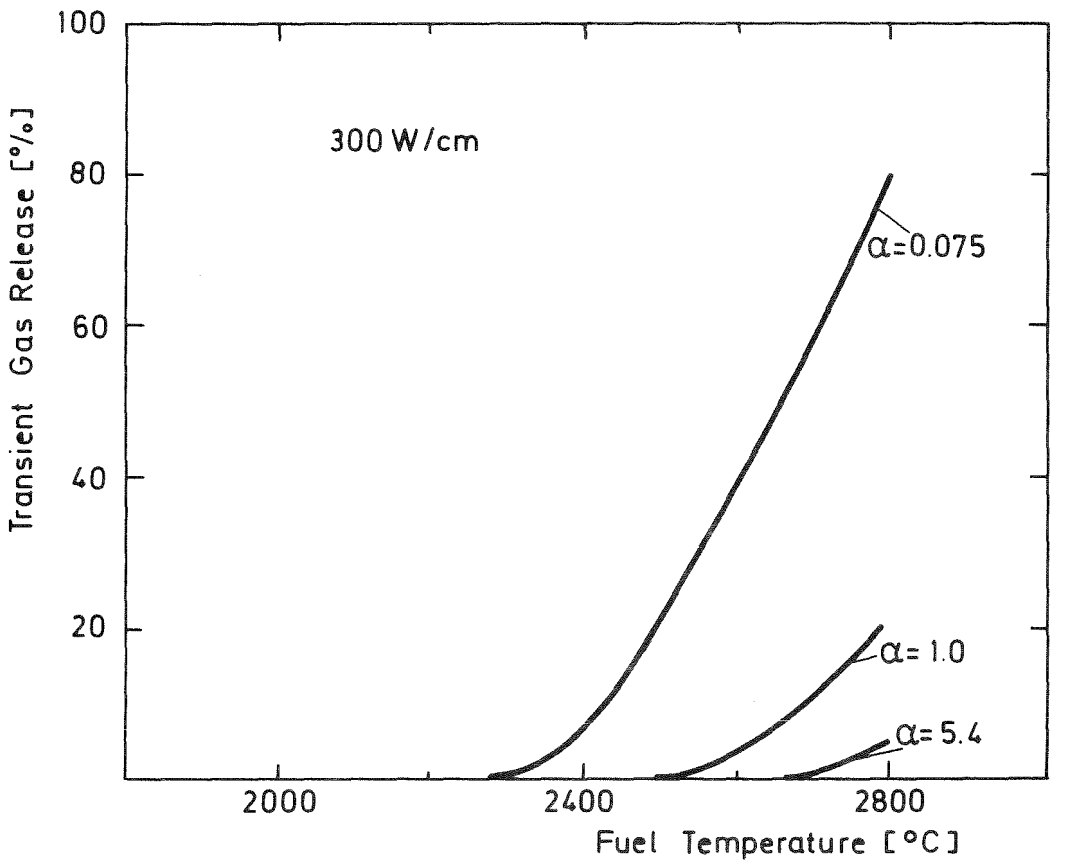

Fig. 12: Transient Gas Release for Different Periods α

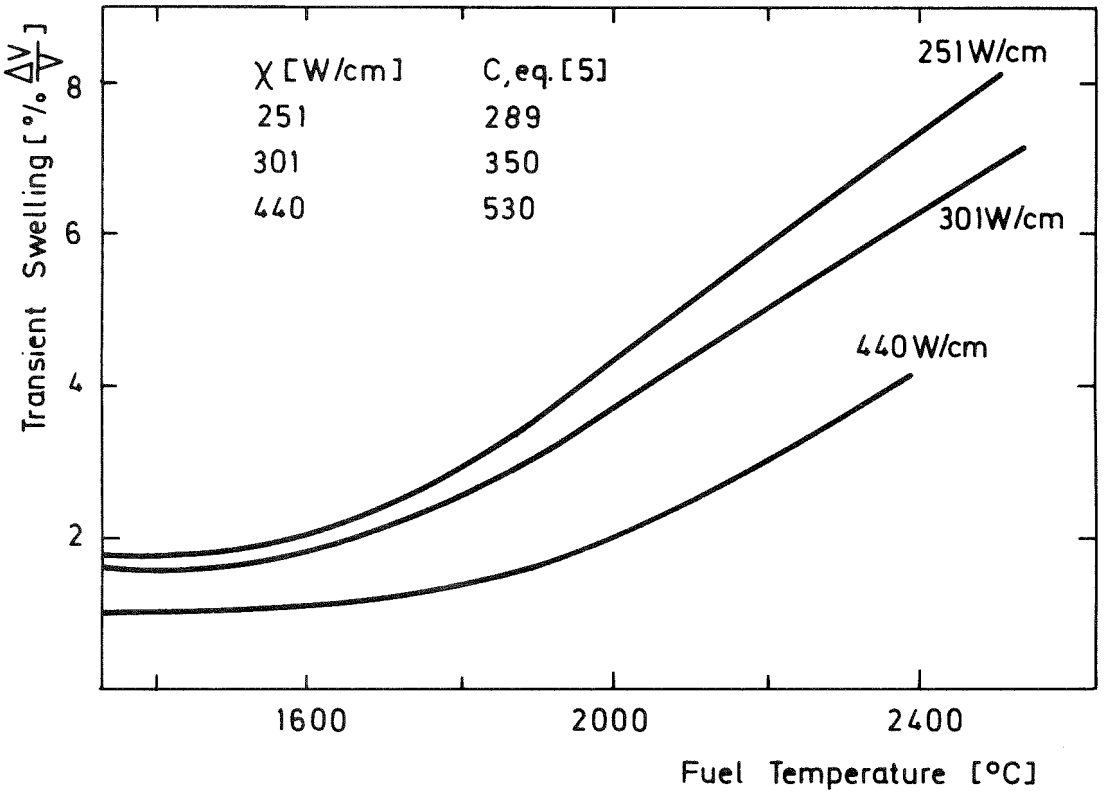

Fig. 13: Transient Swelling (α = 1.0 sec^{-1}) for Different Linear Rod Powers